Development 139, 1095-1104 (2012) doi:10.1242/dev.068569


# The CDC25B phosphatase shortens the G2 phase of neural progenitors and promotes efficient neuron production

**Emilie Peco[1,2,3,4,5,*,‡], Timothé Escude[1,2,*], Eric Agius[1,2], Virginie Sabado[1,2,§], François Medevielle[1,2], Bernard Ducommun[3,4,5] and Fabienne Pituello[1,2,¶]**

## SUMMARY

During embryonic development, changes in cell cycle kinetics have been associated with neurogenesis. This observation suggests that specific cell cycle regulators may be recruited to modify cell cycle dynamics and influence the decision between proliferation and differentiation. In the present study, we investigate the role of core positive cell cycle regulators, the CDC25 phosphatases, in this process. We report that, in the developing chicken spinal cord, only *CDC25A* is expressed in domains where neural progenitors undergo proliferative self-renewing divisions, whereas the combinatorial expression of *CDC25A* and *CDC25B* correlates remarkably well with areas where neurogenesis occurs. We also establish that neural progenitors expressing both *CDC25A* and *CDC25B* have a shorter G2 phase than those expressing *CDC25A* alone. We examine the functional relevance of these correlations using an RNAi-based method that allows us to knock down CDC25B efficiently and specifically. Reducing *CDC25B* expression results in a specific lengthening of the G2 phase, whereas the S-phase length and the total cell cycle time are not significantly modified. This modification of cell cycle kinetics is associated with a reduction in neuron production that is due to the altered conversion of proliferating neural progenitor cells to post-mitotic neurons. Thus, expression of CDC25B in neural progenitors has two functions: to change cell cycle kinetics and in particular G2-phase length and also to promote neuron production, identifying new roles for this phosphatase during neurogenesis.

**KEY WORDS: Embryo, Chicken, Spinal cord, Neurogenesis, Proliferation, Differentiation, CDC25 phosphatases, Cell cycle, G2 phase, Sonic hedgehog**

## INTRODUCTION

A major challenge confronting the developing embryo is that of generating the appropriate numbers and distinct classes of neurons essential for constructing functional neuronal circuits. This involves tight coordination between proliferation, specification and differentiation during the course of neurogenesis. The developing spinal cord is a pertinent model with which to dissect the crosstalk that exists between these different programs, because we have a good understanding of the molecular mechanisms governing spinal neurons specification and differentiation (Dessaud et al., 2008).

The spinal cord develops from a caudal stem zone containing a pool of undifferentiated neural progenitors performing only proliferative divisions, one progenitor generating two daughter progenitor cells (PP) (Akai et al., 2005). Neural progenitors exiting the stem zone to contribute to the formation of the neural tube become subjected to morphogens, including Sonic hedgehog (Shh), which controls their specification, proliferation and survival (Alvarez-Medina et al., 2009; Cayuso et al., 2006; Dessaud et al., 2008; Ulloa and Briscoe, 2007). Neurogenic divisions appear in the closing neural tube concomitantly with the onset of Shh activity (Hammerle and Tejedor, 2007). They are of two types: asymmetric divisions that generate a progenitor and a neuron (PN) and a terminal symmetric division that produces two neurons (NN) (Morin et al., 2007; Wilcock et al., 2007). Although the molecular mechanisms that determine the balance between proliferative and neurogenic divisions are largely unknown, in the spinal cord, the mode of division has been correlated with cell cycle length modifications; the cell cycle of neural progenitors dividing to produce a neuron and a progenitor is longer than that of neural progenitors generating two progenitors (Wilcock et al., 2007).

There is mounting evidence to highlight the role of cell cycle kinetics in controlling the decision of a neural progenitor to proliferate rather than to differentiate, and vice versa. In the amphibian or fish retina, Hedgehog signaling converts slowly dividing stem cells into fast-cycling transient amplifying progenitors, which display shorter G1 and G2 phases, and are about to exit the cell cycle and differentiate (Agathocleous et al., 2007; Locker et al., 2006). During mammalian corticogenesis, a lengthening of G1 phase is associated with neurogenesis, whereas reducing G1-phase length by promoting proliferative divisions is sufficient to decrease neurogenesis (Lange et al., 2009; Pilaz et al., 2009). Cortical progenitors divide into stem-cell-like apical progenitors (AP) and fate-restricted basal progenitors (BP), and extension of G1 phase was recently shown to be associated with the transition from AP to BP progenitors (Arai et al., 2011). AP and BP progenitors committed to differentiation have a shorter S phase than those performing proliferative divisions but an identical G1 phase, suggesting that the lengthening of G1 phase in correlation with neurogenesis reflects the increasing contribution of BPs to neuron production (Arai et al., 2011). These examples illustrate the fact that

[1]Université de Toulouse, CBD, 118 route de Narbonne, F-31062 Toulouse, France. [2]CNRS, CBD-UMR5547, F-31062 Toulouse, France. [3]CNRS, LBCMCP-UMR5088, F-31062 Toulouse, France. [4]CHU de Toulouse, F-31059 Toulouse, France. [5]CNRS, ITAV-UMS3039, F31106 Toulouse, France.

*These authors contributed equally to this work
[‡]Present address: Centre for Research in Neuroscience, McGill University, 1650 Cedar Avenue, Montreal, QC H3G 1A4, Canada
[§]Present address: Department of Craniofacial Development, King's College London Guy's Campus, Guy's Tower Floor 27, London SE1 9RT, UK
[¶]Author for correspondence (fabienne.pituello@univ-tlse3.fr)

**Accepted 9 January 2011**

modifications of cell cycle kinetics can promote neurogenesis, but they also underline the present difficulty of proposing a comprehensive model for the process.

Changing the dynamics of the cell cycle requires recruitment of the core cell cycle machinery, and we therefore hypothesized that specific cell cycle regulators would be used in spinal neural progenitors undergoing proliferative versus neurogenic divisions. Previously, we reported that members of two families of cell cycle regulators, D-type cyclins (cyclinDs) and CDC25 phosphatases, are differentially expressed in the stem zone and in the neural tube. Whereas *cyclin D2* and *CDC25A* are already present in the stem zone, the transcription of *cyclin D1* and *CDC25B* is initiated when Shh signaling is turned on, suggesting that this morphogen controls the expression of a specific set of cell cycle regulators in order to adapt proliferation to neurogenesis (Alvarez-Medina et al., 2009; Benazeraf et al., 2006; Lobjois et al., 2004; Ulloa and Briscoe, 2007).

In mammals, the CDC25 family is composed of three members, *CDC25A*, *CDC25B* and *CDC25C*. Only *CDC25A* and *CDC25B* are found in the chicken genome. CDC25 phosphatases are positive regulators of cell cycle phase transitions, given that they activate cyclin-dependent kinase (CDK) complexes (Boutros et al., 2007). CDC25A is implicated in the control of G1-S and G2-M transitions by regulating the activities of CDK1 and CDK2, whereas CDC25B seems to be mainly involved in activating CDK1-cyclin B at the G2-M transition (Boutros et al., 2007; Timofeev et al., 2009; Timofeev et al., 2010). Interestingly, in *C. elegans* embryos, different levels of CDC25 phosphatase may account for differences in cell cycle length (Rivers et al., 2008). This raises the possibility that the combined activities of CDC25B and CDC25A in neural progenitors may modify cell cycle characteristics and influence neuronal differentiation.

In this study, we report first that the combinatorial expression of *CDC25A* and *CDC25B* correlates with neurogenesis during spinal cord development, and, second, that downregulating *CDC25B* impedes neuron production by altering the conversion of progenitor cells to post-mitotic neuron, thus revealing a new role for this CDC25B phosphatase during neurogenesis. We also establish that neural progenitors expressing both *CDC25A* and *CDC25B* have a shorter G2 phase than those expressing *CDC25A* alone. Moreover, downregulation of CDC25B results in a lengthening of the G2 phase without significant modification of the S phase or total cell cycle duration. Together, these data lead us to propose a new model whereby Shh, through increasing the level of CDC25B phosphatase in neural progenitors, alters two processes: (1) cell cycle kinetics (in particular G2-phase length) and (2) neuron production.

## MATERIALS AND METHODS

### Embryos

Fertile hens' eggs were incubated at 38°C in a humidified incubator to yield embryos appropriately staged (Hamburger and Hamilton, 1992).

### DNA constructs and in ovo electroporation

Gain-of-function experiments were performed using a bi-cistronic vector expressing the human CDC25B3 isoform and EYFP under the control of a CMV promoter. For the loss-of-function experiments, we used the pRFPRNAiA vector (Das et al., 2006) in which we replaced RFP with GFP or H2B-RFP. Targeted sequences were as follows: CDC25B, 5′-AAGATCATCACAGACAAGAAGT-3′ and 5′-AGGAGGATGACG-GCTTCATGGA-3′; scramble, 5′-GCGGTTACGTGCGATAGGAGAA-3′. 'Control vector' designates empty pGFPRNAiA derived from pRFPRNAiA (Das et al., 2006). In ovo electroporation experiments were performed as described previously (Lobjois et al., 2004) using 1.5- to 2-day-old chicken embryos. We initially electroporated CDC25B-RNAi from 0.5 to 2 μg/μl to define the lowest dose (0.8 μg/μl) that significantly reduced the level of *CDC25B* transcripts as visualized by in situ hybridization.

### In situ hybridization and immunohistochemistry

Transcripts were detected on 40 μm vibratome sections, as previously described (Benazeraf et al., 2006; Lobjois et al., 2008; Lobjois et al., 2004). For double in situ hybridization, *NeuroM* and *CDC25B* antisense RNA probes were labeled using DIG and Fluo-RNA labeling mix, respectively (Roche), as described previously (Pituello et al., 1995). The antibodies used in the present studies are: anti-Pax7, anti-BrdU (mouse monoclonal, G3G4), anti-Islet1/2, anti-Lim1/2, anti-MNR2 (Hybridoma Bank), anti-Flag (Sigma), anti-Actin and anti-Sox2 (Chemicon), anti-P-H3 (Upstate Biotechnology), anti-HuC/D (Molecular Probes), anti-GFP (Torrey Pines Biolabs), anti-Olig2 (Chemicon), anti-neuronal class III β-tubulin (Tuj1, BAbCO), anti-$p27^{kip1}$ (BD Biosciences), anti-BrdU (rat anti-BrdU, AbD Serotec), anti-MPM2 (Upstate Biotechnology), and anti-NeuroM (a gift from J. Muhr, Karolinska Institutet, Stockholm, Sweden).

### Western blotting

Western blots were performed using 12 neural tubes dissected from embryos harvested 24 hours after co-electroporation of CDC25B-RNAi or of control RNAi from a plasmid encoding a modified form of the chicken chCDC25B3 with a Flag at the end of the catalytic C-terminal domain (pECE-chCDC25B3Flag-IRES-GFP) (Bel-Vialar et al., 2007). Dissected neural tubes were selected on red fluorescence intensity and cell extracts were obtained by lyzing the explants in Laemmli 1× buffer. Proteins were separated using NuPAGE gels (Invitrogen) and transferred to nitrocellulose membrane. Immunodetection was performed using anti-Flag (1/1000) or anti-actin (1/10,000) antibodies.

### Cell proliferation and survival analyses

Cell proliferation was evaluated by incorporation of bromodeoxyuridine (BrdU, Sigma, St Louis, MO, USA): 10 μl of 48 mM BrdU solution were injected into embryos harvested 30 minutes or 1 hour later, and BrdU immunodetection was performed on vibratome sections (Lobjois et al., 2004). Mitotic cells were detected using anti-P-H3 or anti-MPM2 antibodies. G2-phase length was determined using the percentage of labeled mitoses (PLM) paradigm (Quastler and Sherman, 1959). BrdU incorporation was performed as described above, except that a similar dose of BrdU was added every 2 hours, and embryos were harvested from 30 to 180 minutes later. Embryos were fixed and labeled for both BrdU and P-H3. We then quantified the percentage of P-H3 and BrdU co-labeled nuclei with increasing times of exposure to BrdU. The progression of this percentage is proportional to G2-phase duration. Determination of S-phase length (Ts) and total cell cycle length (Tc) was based on the relative numbers of cells that incorporated one or both of the thymidine analogs (Martynoga et al., 2005). In ovo BrdU (500 μM) incorporation was followed after 90 minutes by EdU (500 μM, Invitrogen) incorporation and embryos were fixed 30 minutes later. EdU was detected first (Click-iT EdU Alexa Fluor 647 Imaging Kit, Invitrogen), followed by BrdU detection as described above using the G3G4 antibody that does not recognize EdU. Quantification was performed on the proliferating fraction of the RFP+ population, which was obtained by subtracting the percentage of HuC/D+/RFP+ differentiated cells observed on serial sections, from the total number of RFP+-transfected cells. BrdU+ and EdU+ cells (those remaining in S-phase at the end of the experiment), and BrdU+ and EdU– cells (those in S phase when BrdU was applied, but had left S prior to EdU incorporation) were counted. The length of S-phase, Ts, was calculated as the interval between BrdU and EdU injections (90 minutes) multiplied by the quotient of BrdU+/EdU+ cells and BrdU+/EdU– cells. The total cell cycle length (Tc) was evaluated by multiplying Ts by the quotient of RFP+/HuC/D– cells and BrdU+/EdU+ cells.

For birthdating experiments, 10 μl of a 500 μM EdU solution were applied once on the heart of embryos 15 hours or 63 hours after electroporation. In our experimental conditions, only cells undergoing S phase during approximately the following 2 hours were labeled, enabling us to count only neurons that are newly born during this time. Embryos were fixed 33 hours later, processed for sectioning and stained as described above.

Cell death was analyzed by TUNEL assay, using the 'In Situ Cell Death Detection Kit TMR red' (Roche, Basel, Switzerland) and by immunofluorescence, using the anti-active caspase 3 monoclonal antibody

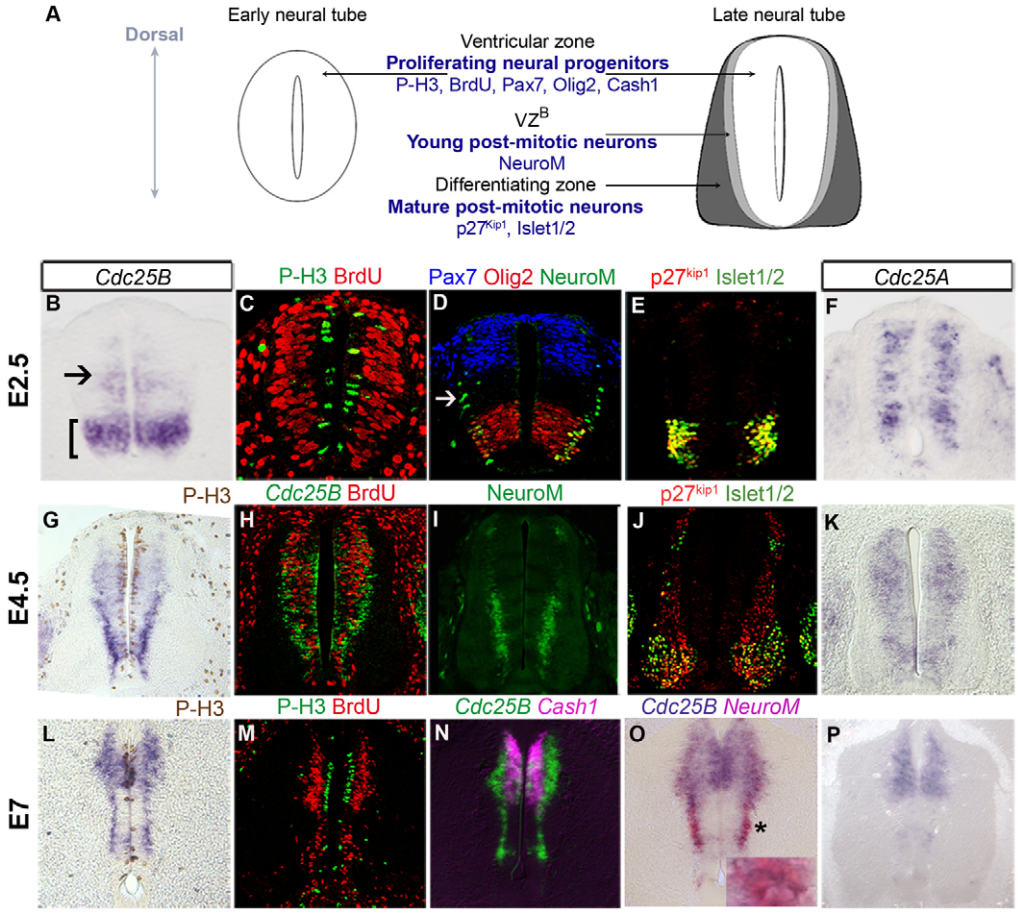


**Fig. 1. *CDC25B* expression correlates with neurogenic domains during chicken spinal cord development.**
(**A**) Schematic representation of a cross-section of the chick neural tube at E2.5 (left) and E4.5 (right), illustrating the organization of the structure and the position of the different markers used. (**B-P**) Cross-sections of the spinal cord at E2.5 (B-F), E4.5 (G-K) and E7 (L-P). In situ hybridization of *CDC25B* (B,G,H,L,N,O), *CDC25A* (F,K,P), *Cash1* (N) and *NeuroM* (O). The inset in O is a higher magnification at the level of the asterisk and shows two cells co-expressing *CDC25B* (blue) and *NeuroM* (red). Immunodetection of P-H3 (C,G,L,M), BrdU (C,H,M), NeuroM (D,I), Pax7 (D), Olig2 (D), $p27^{Kip1}$ (E,J) and Islet1/2 (E,J). Arrows in B and D show *CDC25B* and NeuroM dorsal progression, respectively.

(BD Biosciences). To quantify immunolabeled cells in the transfected population, we either used the GFP of the pGFPRNAi vector or co-electroporated a pCS-Histone2B-mRFP vector (a gift from X. Morin, Ecole Normale Supérieure, Paris, France).

### Imaging and data analysis

Slices (40 µm) were analyzed using an epifluorescence Nikon microscope or a SP2 Leica confocal microscope as described previously (Benazeraf et al., 2006; Lobjois et al., 2008). Experiments were performed in duplicate or, most often in triplicate, with two or three embryos per experiment. For each embryo, confocal analyses were performed on three to five 40 µm slices. Confocal images were acquired throughout the slices at 3 µm *z* intervals, thus avoiding the inclusion of the same nucleus in two consecutive images. Quantifications were performed using the Metamorph software on at least three confocal sections (0.7 µm axial resolution) per 40 µm slice. When quantification was performed by cell counting, only one of the three sections was used to avoid counting the same cell twice. The effects of CDC25B-RNAi on Tuj1 protein and on Pax6 expression were quantified using Image J Tool software.

The normality of the data sets was determined, analyses of variance performed and the appropriate T-test method used. Values shown are mean ± standard error of the mean (s.e.m.). The significance values are: $*P<0.05$; $**P<0.01$; $***P<0.001$.

## RESULTS

### *CDC25B* expression correlates temporally and spatially with neuron production in the developing spinal cord

To characterize the role of CDC25 phosphatases during neurogenesis, we analyzed by in situ hybridization the kinetics of *CDC25B* and *CDC25A* expression at different milestones of spinal cord development. At E2.5 (HH stage 16-17), which corresponds to a peak period of motoneuron (MN) production in the ventral neural tube, *CDC25B* transcripts are detected in a restricted domain located in the ventralmost region of the neural tube (Fig. 1A,B, bracket in B). Faint staining is also observed along the lumen (arrow, Fig. 1B). At this stage, intense proliferation occurs throughout the neural tube, as visualized by BrdU incorporation and phospho-histone 3 (P-H3) immunostaining (Fig. 1C). *CDC25B* is thus present in only a subset of proliferating neural progenitors. The domain of high *CDC25B* expression contains progenitors of motoneurons (pMNs) that express Olig2 (Fig. 1B,D). pMNs are intensively producing MNs, as visualized using p27Kip1 (post-mitotic cells) and the pan-MN marker Islet1/2 (Fig. 1E). The presence of *CDC25B* transcripts along the lumen (arrow, Fig. 1B) accompanies the dorsal expansion of NeuroM, which transiently marks young post-mitotic neurons, indicating the progression of neurogenesis (arrow, Fig. 1D). The domain of dorsal progenitors defined by Pax7 expression (Fig. 1D), which produces few, if any, neurons at E2.5 (p27Kip1 Fig. 1E, see also HuC/D immunostaining Fig. 5F) does not express *CDC25B* (Fig. 1B,D). This analysis reveals that *CDC25B* is strongly expressed in domains where neuronal production takes place.

At E4.5, there is a notable change in *CDC25B* expression; intense staining is observed on the basal side of the ventricular zone ($VZ^B$), which extends dorsally (Fig. 1G-H) and concomitantly with NeuroM dorsal progression and neuron production (Fig. 1I,J). At E7, *CDC25B* is strongly expressed in dorsal neural progenitors that express the proneural gene *Cash1* (Fig. 1L,N). This dorsal

domain is a site of intense proliferation (Fig. 1L,M) and neuron production (Fig. 1O). Double in situ hybridization performed at E7 reveals that *CDC25B*-VZ$^{B}$ and *NeuroM* domains overlap, suggesting that *CDC25B* expression persists transiently in young post-mitotic neurons (Fig. 1O). At E7, the Olig2+ domain has switched to the generation of oligodendrocytes (Rowitch, 2004), and *CDC25B* is not detected in the ventral-most progenitors (Fig. 1N-O). These data underline the excellent spatial and temporal correlation between the dynamics of CDC25B expression and neurogenesis.

The dynamics of *CDC25A* expression reveals that at E2.5 and E4.5, high levels of *CDC25A* are detected throughout the VZ, which contains numerous proliferating neural progenitors (Fig. 1F,K). At E7, transcripts are mainly detected in the dorsal one-third of the neural tube, in which intensive proliferation is observed (Fig. 1M,P). These data indicate that *CDC25A* is expressed in domains of high proliferation, whereas the domains where *CDC25A* and *CDC25B* are co-expressed correspond to areas where neurogenesis occurs.

## CDC25B downregulation impedes neuron production

This strong correlation between *CDC25B* expression and neurogenic domains prompted us to determine whether CDC25B plays a role in neuron production. We performed gain-of-function experiments by misexpressing human CDC25B in the chicken neural tube. Within 6 hours the percentage of mitotic cells rises from 4.69±0.55% to 15.74±2.73% (mean±s.e.m.) in embryos electroporated with a control vector ($n$=3 embryos) compared with embryos overexpressing CDC25B ($n$=3 embryos; $P$=0.027; supplementary material Fig. S1A,B,E), leading to mitotic catastrophe and subsequent apoptosis (supplementary material Fig. S1C,D,F) as previously observed (Bugler et al., 2010; Karlsson et al., 1999; Lobjois et al., 2009). Although this experiment shows that CDC25B functions at the G2-M transition, this drastic effect limits its use to decipher the precise role of CDC25B during neurogenesis. Consequently, we turned to knockdown experiments, using in ovo electroporation of a microRNA (RNAi)-based vector (Das et al., 2006). Four RNAis directed against CDC25B were designed, and two of them efficiently reduced the amount of *CDC25B* mRNA, one being particularly effective both on the transcript and on the protein (Fig. 2A,A′; supplementary material Fig. S2). After ensuring that these CDC25B-RNAis did not alter *CDC25A* expression (Fig. 2B) and that a scramble-CDC25B-RNAi did not modify *CDC25B* expression (Fig. 2C,C′), we mainly used the most efficient CDC25B-RNAi to knock down CDC25B.

To determine the effect of downregulating CDC25B on neurogenesis, we analyzed neuron production using *NeuroM* as a marker of young neurons, and p27$^{Kip1}$ or the pan-neuronal marker TuJ1 for post-mitotic differentiated neurons. Forty-eight hours after electroporation of *CDC25B*-RNAi, we observed a marked reduction of *NeuroM* transcripts on the electroporated side of the neural tube ($n$=9/10 embryos) (Fig. 2D-E′). p27$^{Kip1}$ and Tuj1 staining were also clearly reduced on the side transfected with *CDC25B*-RNAi (Fig. 2H-I″). We quantified the effect by measuring the size of Tuj1-positive areas on the electroporated (EP) side and comparing it with the non-electroprated side (NEP). As shown on the histogram in Fig. 2L, misexpressing a control-RNAi does not diminish the Tuj1+ area, whereas CDC25B-RNAi

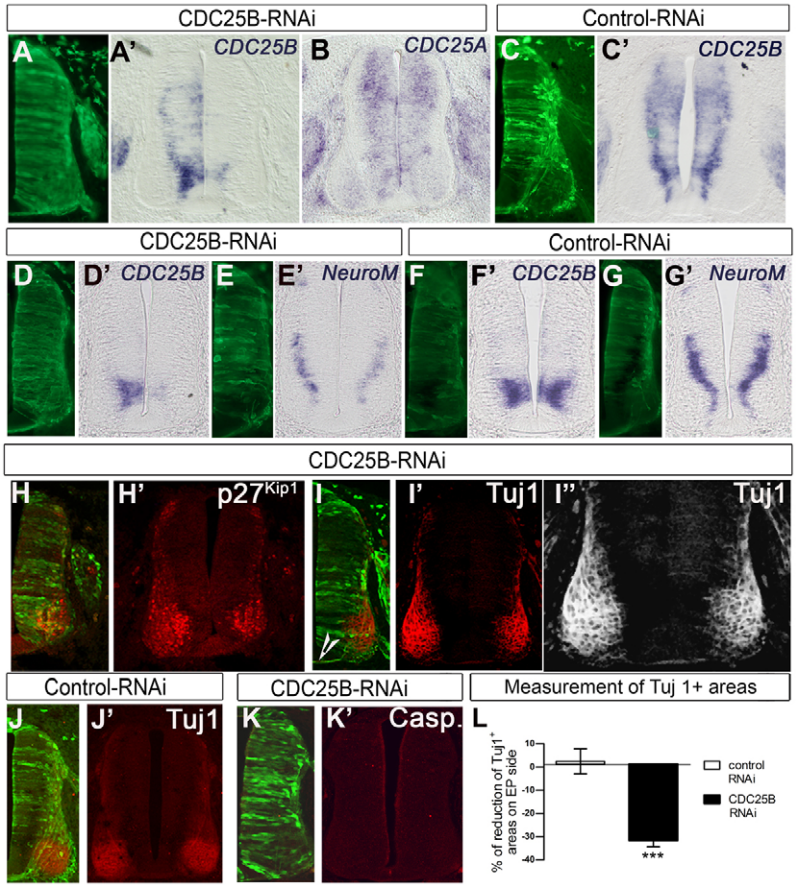


**Fig. 2. *CDC25B* downregulation impedes neuronal differentiation.** (**A-K′**) Cross-sections of the chick spinal cord at E3.5-E4, 48 hours after electroporating CDC25B-RNAi (A-B,D-E′,H-I″,K-K′) or a control-RNAi (C,C′,F-G′,J-J′). In situ hybridization showing the reduction of *CDC25B* (A′,D′) and *NeuroM* (E′) but not of *CDC25A* transcripts (B). Immunodetection of p27$^{Kip1}$ (H,H′), Tuj1 (I,I′,I″), active caspase 3 (K,K′) following electroporation of CDC25B-RNAi. Arrowhead in I shows labeled neuritic processes. Electroporating a control RNAi had no impact on *CDC25B* (F,F′), *NeuroM* (G,G′) or Tuj1 (J,J′). Transfected cells are visualized with GFP (green). (**L**) The histogram represents the surface covered by Tuj1 immunoreactivity measured using Image Tool software on control- (red) compared with CDC25B-RNAi (green) electroporated embryos. ***$P$<0.001.

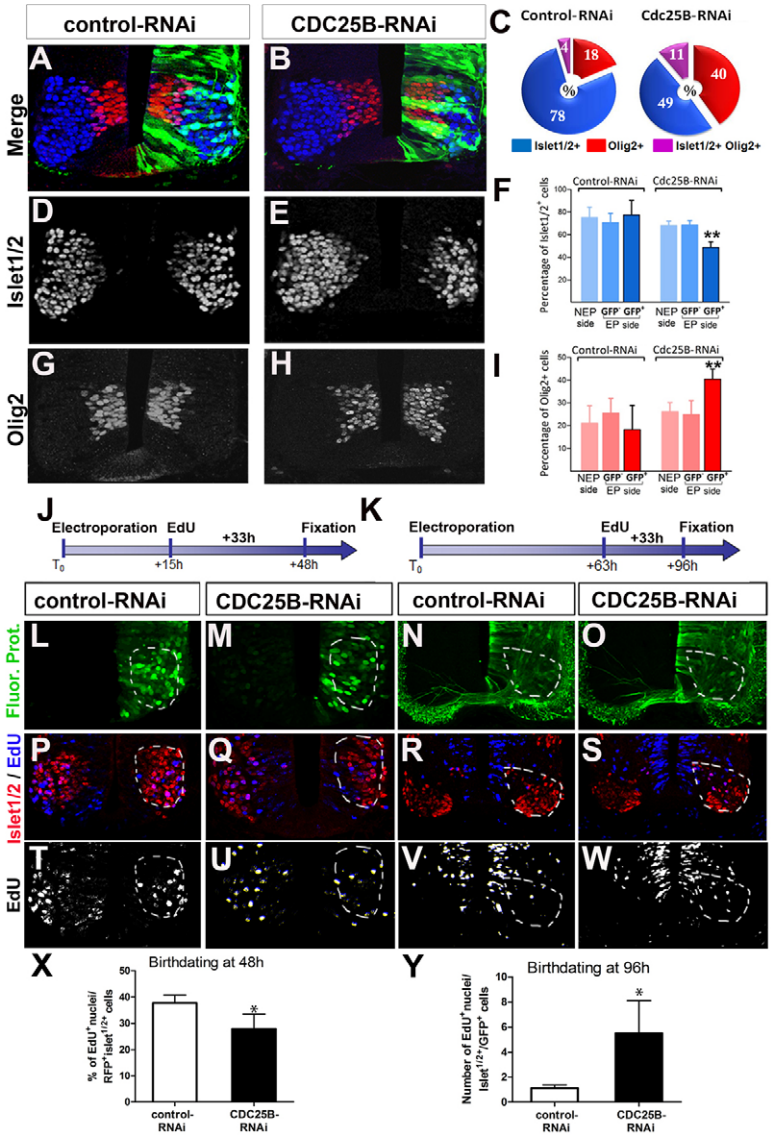


**Fig. 3. *CDC25B* downregulation delays MN differentiation by retaining neural progenitors in the progenitor state.** (**A**,**B**,**D**,**E**,**G**,**H**) Cross-sections of the spinal cord of E3.5-E4 chick embryos 48 hours after electroporation of a control- (A,D,G) or CDC25B- (B,E,H) RNAi, showing the GFP+ electroporated cells (A,B, in green), Islet1/2+ (A,B, in blue; D,E), Olig2+ (A,B, in red; G,H) cells. (**C**,**F**,**I**) Distribution of control- and *CDC25B*-RNAi transfected GFP+ cells: Islet1/2+ (blue), Olig2+ (red) and Islet1/2/Olig2+ (pink) based on quantifications detailed in F and I, performed on the non-electroporated side (NEP) and the GFP– and GFP+ populations of the electroporated side (EP). The analysis was quantified by counting the total number of Islet1/2+, Olig2+ and Islet1/2+/Olig2+ cells in each population (NEP, GFP- or GFP+) and defining the distribution of cells expressing each marker as a percentage of the total population. Quantifications were carried out on over 2250 cells for each histogram on six and five embryos for the *CDC25B*-RNAi and the control-RNAi vector, respectively. Error bars represent 95% confidence intervals. (**J**,**K**) Schematic representation of EdU birthdating experiments. (**L-Y**) Cross-sections of the spinal cord of embryos 48 hours (L,M,P,Q,T,U) or 96 hours (N,O,R,S,V,W) after electroporation of a control- (L,N,P,R,T,V) or CDC25B- (M,O,Q,S,U,W) RNAi, showing the electroporated cells [L-O, in green (L-M, false color for RFP), Islet1/2 (P-S, in red), EdU (P-S in blue; T-W)]. The histograms represent the quantification of the EdU+/Islet1/2+ expressed as a percentage of transfected cells (X) or as the mean number of EdU+/Islet1/2+/GFP+ nuclei on the EP side (Y). Pictures represent *z* sections obtained with a confocal microscope. h, hours. **P*<0.05, ***P*<0.01.

results in a 31.6±1.41% reduction ($n$=37 sections from three embryos, $P$<0.001). We clearly observed GFP+/p27$^{Kip1}$+ cells and GFP+ neuritic processes growing from transgenic cells located in the mantle zone (Fig. 2, arrowhead in I), indicating that some transfected CDC25B-RNAi cells were able to exit the cell cycle and differentiate. Mis-expressing a scramble- or control-RNAi had no effect either on *NeuroM* (Fig. 2F-G′), or on Tuj1 (Fig. 2J,J′) or p27$^{Kip1}$ expression (data not shown). This decrease in differentiating neurons was not due to enhanced cell death, as we did not observed an increase in active caspase 3 or TUNEL assay staining on the CDC25B-RNAi-transfected side compared with the contralateral control side 24 or 48 hours after electroporation (Fig. 2K,K′; data not shown). These observations indicate that downregulating CDC25B affects neuronal production.

## CDC25B downregulation inappropriately maintains neural cells in the progenitor state at the cost of neuronal differentiation

MNs differentiate from the Olig2 domain of progenitors showing high levels of *CDC25B*, as illustrated in Fig. 1B,D,E. To establish further the role of CDC25B in neuron production, we asked whether the absence of CDC25B had any effects on the sequence of events leading to the genesis of MNs. We analyzed the distribution of control- and CDC25B-RNAi-transfected GFP+ cells 48 hours after electroporation by quantifying the percentage of cells: (1) in the differentiated state (Islet1/2+ cells), (2) in the progenitor state (Olig2+) and (3) in a subset of cells co-expressing both markers (Olig2+ and Islet1/2+ cells) (Fig. 3).

We found that 77.4±6.4% of control-GFP+ cells express Islet1/2, whereas the percentage drops down to 48.7±2.5% ($P$=0.007) in cells transfected with CDC25B-RNAi, corresponding to a reduction of 37% in the number of neurons (Fig. 3A-F), confirming our previous results that CDC25B downregulation impedes neuron production (Fig. 2H′,I′,I″). Remarkably, the percentage of Olig2+ cells shifted from 18.3±5.3% in control-GFP+ cells to 40.5±2.2% ($P$=0.01) in CDC25B-RNAi GFP+ cells, i.e. a 121% increase (Fig. 3A-C,G-I). When Olig2+ CDC25B-RNAi transfected cells were subjected to a 1-hour BrdU pulse, 44.81±3.14% of Olig2+/RFP+ cells had incorporated BrdU, showing that the cells had not stopped proliferating. These observations indicate that the reduction in neurons production following CDC25B downregulation is due to the maintenance of neural progenitors in the progenitor state. We also observed a clear difference in the percentage of cells co-expressing Olig2 and Islet1/2 (4.3±1.1% control-RNAi versus

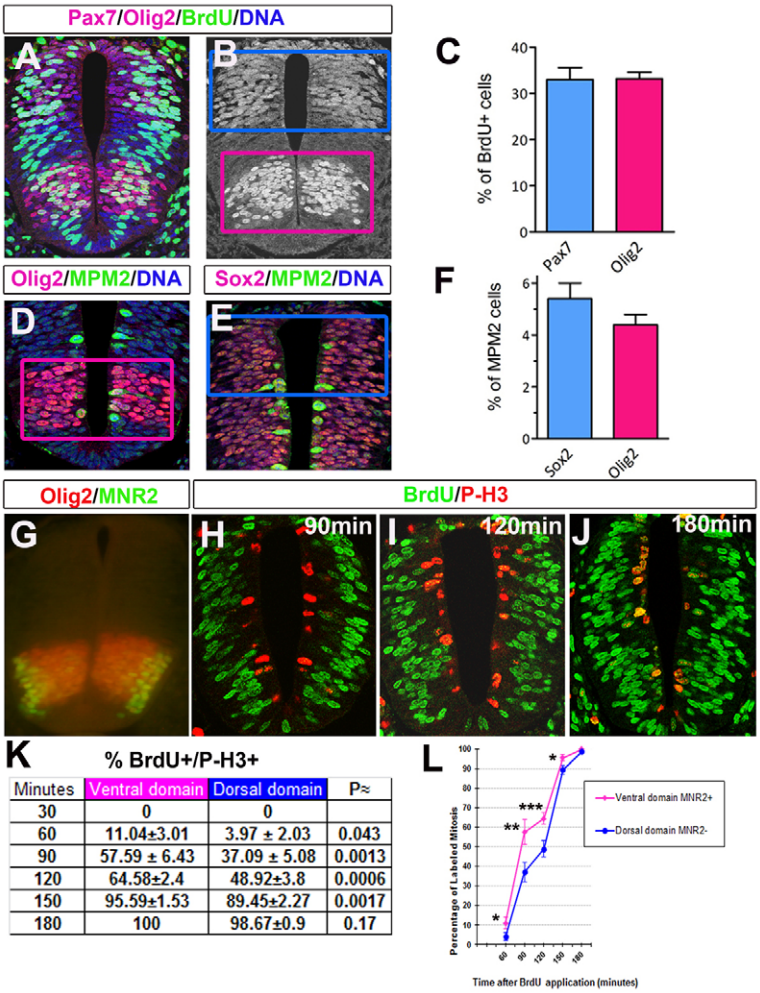


| Minutes | Ventral domain | Dorsal domain | P≈ |
|---|---|---|---|
| 30 | 0 | 0 | |
| 60 | 11.04±3.01 | 3.97 ± 2.03 | 0.043 |
| 90 | 57.59 ± 6.43 | 37.09 ± 5.08 | 0.0013 |
| 120 | 64.58±2.4 | 48.92±3.8 | 0.0006 |
| 150 | 95.59±1.53 | 89.45±2.27 | 0.0017 |
| 180 | 100 | 98.67±0.9 | 0.17 |

**Fig. 4. Ventral and dorsal progenitors display different G2-phase length.** (**A**,**B**,**D**,**E**) Cross sections of the chick spinal cord of E2,5 chicken embryos. S-phase cells were identified by immunostaining for BrdU (A,B, green) and mitotic cells by MPM2 labeling (D,E, green). The ventral progenitor domain is visualized with Olig2 staining (A,B,D; Olig2 and pink rectangle) and the dorsal progenitor domain (B,E blue rectangle) either with Pax7 (A,B) or Sox2 (E). (**C**,**F**) Quantification of the percentage of BrdU+ cells following a 30-minute pulse (C) and of MPM2+ cells (F) in the dorsal (blue) and ventral (pink) progenitor domains. (**G**) Immunostaining showing Olig2 (red) and MNR2 (green); marker used here to determine the position of the domain of ventral progenitors. (**H-J**) Examples of the double BrdU/P-H3 immunostaining observed at different time-points after BrdU incorporation every 2 hours and used to estimate the length of the G2 phase. (**K**) Values obtained from three independent experiments at each time-point. (**L**) The progression of the number of BrdU/P-H3 co-labeled nuclei with increasing BrdU exposure times. Error bars represent 95% confidence intervals (C,F) or s.e.m. (L). **P*<0.05, ***P*<0.01, ****P*<0.001.

10.8±1.5% CDC25B-RNAi; *P*=0.008) (Fig. 3C), which may simply reflect the increase in the Olig2+ population, as there is no difference in the ratio of Olig2+Islet+ and Olig2+ cells between the control and the CDC25B-RNAi-transfected populations (0.23±0.03 versus 0.27±0.05; *P*=0.76). Non-transfected cells on the electroporated side behave as cells of the contralateral non electroporated side (Fig. 3F,I), indicating that the effect of CDC25B on cell differentiation is cell autonomous. Together these data indicate that CDC25B downregulation hinders neuronal differentiation by retaining neural progenitors in the progenitor state.

If this assumption is true, restoring normal levels of *CDC25B* should enhance neuronal production. We tested this prediction by taking advantage of the temporal effect of the RNAi-mediated downregulation of CDC25B. Maximum efficiency of RNAi was observed between 15 and 48 hours after electroporation (data not shown and Fig. 2D′) but 3 days after electroporation its effect had lessened, owing to plasmid dilution through cell divisions. We thus performed birthdating experiments at two time points: at 15 hours, when CDC25B is strongly downregulated; and 3 days after electroporation, when *CDC25B* expression has recovered (supplementary material Fig. S3G). EdU was applied only once to the developing embryo and we counted the intense labeled nuclei that represent neurons born just after the time of EdU injection. When EdU was applied 15 hours after electroporation and neurons born at the time of EdU injection were assessed 48 hours after electroporation (Fig. 3J), we observed a significant reduction in the number of EdU+/Islet1/2+/RFP+ cells in the CDC25B RNAi transfected cells versus the control cells (27.9±2.8% versus 36.7±1.5%, *P*=0.03) (Fig. 3L-X). When EdU was administrated 63 hours after electroporation, followed by an assessment of the EdU+/Islet1/2+/GFP+ cells 33 hours later (Fig. 3K), we observed 5.5±1.3 EdU+/Islet1/2+/GFP+ nuclei on the electroporated side of embryos transfected with CDC25B-RNAi, whereas only rare EdU+ transfected cells (1.1±0.13; *P*=0.02) were detected on embryos electroporated with a control-RNAi vector, or on the non electroporated side (Fig. 3N-Y). These data reinforce our conclusion that the effect of CDC25B on neuron production is due to the maintenance of neural progenitors in the progenitor state, thereby delaying their differentiation.

Because CDC25B expression progresses from ventral to dorsal as the neural tube develops (Fig. 1B,G,L), we wondered whether other populations of neurons located dorsal to the MNs were also affected by CDC25B downregulation. We observed a significant reduction of the Lim1/2+ population of interneurons located just above the MN area in embryos electroporated with CDC25B-RNAi compared with control (0.86±0.01 versus 1.015±0.03, ratio EP/NEP side, *P*<0.001; supplementary material Fig. S3C,C′). The reduction of Lim1/2+ neurons is associated with an increase of Pax6+/GFP+ immunoreactivity (supplementary material Fig. S3I-M), indicating again that cells transfected with CDC25B-RNAi are retained in the progenitor state. At that stage, the analysis of

Lim1/2 expression revealed that the Lim1/2+ cells located in the MNs domain were absent after knock down of CDC25B (supplementary material Fig. S3C-E′). These cells correspond to the late-born lateral motor column (LMC), the temporal formation of which is well established, beginning at stage 21 (corresponding to E3.5) (Sockanathan and Jessell, 1998). One day later, we observed a rescue of *CDC25B* expression that was associated with the presence of $LMC_L$ cells, albeit fewer in number (supplementary material Fig. S3F-H), confirming the effect of CDC25B downregulation on the time-course of neuron production.

Together, these observations show that *CDC25B* downregulation results in the maintenance of neural progenitors in the progenitor state at the expense of neuron production, indicating that CDC25B regulates the balance between progenitor and differentiating states.

## Neural progenitor domains expressing a high level of CDC25B display a shorter G2 phase

Because CDC25 phosphatases are positive regulators of the transitions between cell cycle phases, we first asked whether progenitor domains expressing different combination of CDC25 phosphatases display distinct cell cycle kinetics. We compared in E2-E2.5 embryos the cell cycle parameters in the ventral Olig2+ domain that expresses both *CDC25A* and *CDC25B*, and in a dorsal domain (visualized with Pax7+ or equivalent) that expresses mainly *CDC25A* (Fig. 4). In a population of asynchronously cycling cells, the fraction of cells in a given phase of the cell cycle is proportional to the length of that phase, relative to the total length of the cell cycle. We first determined the fraction of cells in S phase by applying a 30-minute BrdU pulse. We did not find any difference between the Olig2+ and Pax7+ domains that display 33.03±1.3% and 33.22±0.7% BrdU+ cells, respectively (Fig. 4A-C). Then, the fraction of mitotic cells was assessed by using the MPM2 marker in the Olig2+ ventral domain and in a dorsal domain of progenitors, defined by Sox2+ expression, corresponding to that of the Pax7 domain in position and size (Fig. 4D,E). There was no significant difference in the mitotic index of these domains (i.e 4.39±0.2% in Olig2+ domain and 5.04±0.3% in the dorsal Sox2+ domains; $P$=0.12) (Fig. 4F). We next compared the length of the G2 phase in the ventral versus the dorsal neural tube using the percentage of labeled mitosis (PLM) method (Quastler and Sherman, 1959). Embryos were injected with BrdU and allowed to recover for 30 to 180 minutes before fixing and staining with anti-BrdU and P-H3 antibodies. The position of the ventral domain was determined using MNR2 as a marker; for the dorsal domain, one-third of the dorsal neural tube without the roof plate was analyzed (Fig. 4G-J). We found that the percentage of P-H3/BrdU positive cells is consistently lower in the dorsal domain than in the ventral domain (Fig. 4K,L). The average G2 lengths of ventral and dorsal progenitors calculated from the curve are 1 hour 25 minutes and 2 hours 2 minutes, respectively (Fig. 4L). This indicates that progenitors in the ventral domain have a shorter G2 phase than those in the dorsal domain. As *CDC25B* and *CDC25A* are both expressed in this ventral domain, this result strongly suggests that their combined activity leads to a shortening of the G2 phase.

## Downregulating CDC25B in neural progenitors results in a lengthening of the G2-phase

Our observation that neural progenitors located in a domain expressing a high level of CDC25B display a shorter G2-phase length prompted us to determine whether CDC25B could influence

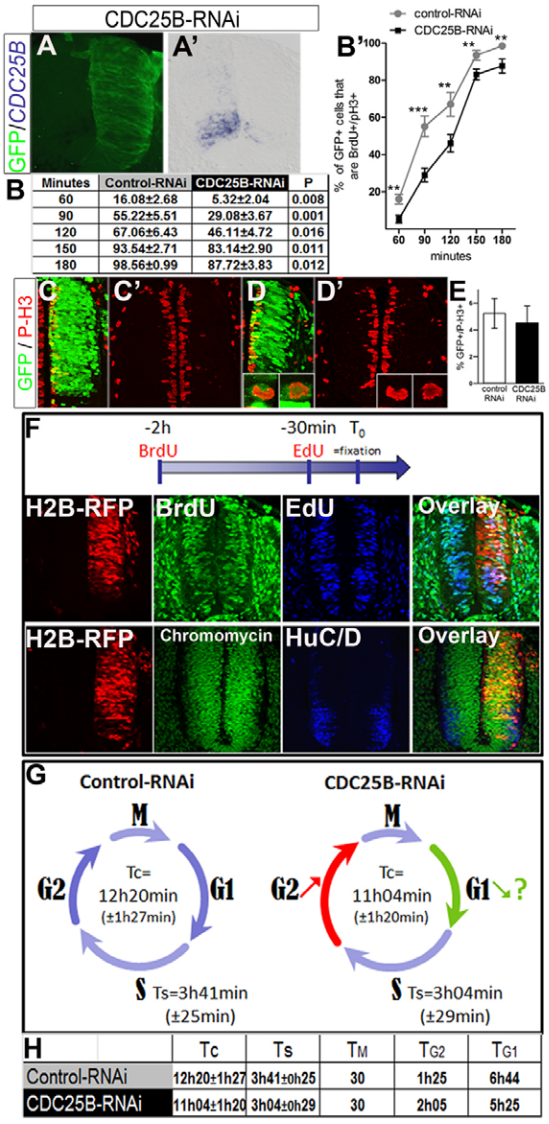


**Fig. 5. Downregulating CDC25B affects the G2-phase length.** (**A**,**A′**) Cross-sections for the chick neural tube at E2.5; in situ hybridization showing the downregulation of *CDC25B* 24 hours after expressing the CDC25B-RNAi. (**B**,**B′**) Quantification of the percentage of GFP+ cells that are BrdU+/P-H3+ following electroporation of CDC25B-RNAi or a control vector (illustrated as a curve in B′). Error bar represents s.e.m. For each point, quantification was performed on four or five embryos for CDC25B-RNAi and three or four embryos for the control vector. (**C-D′**) Analyses of PH-3 immunostaining on cross-sections of the spinal cord 24 hours after electroporating a control vector (C,C′) or *CDC25B*-RNAi (D,D′). Transgenic cells in mitosis are shown at higher magnification in insets in D and D′. (**E**) A quantification performed on over 10,000 cells from three embryos for *CDC25B*-RNAi (green) and two embryos for the control-RNAi vector (red). Error bars represent 95% confidence intervals. (**F**) Representation of the double S-phase labeling technique performed to estimate the length of S-phase (Ts) and the total cell cycle (Tc). Pictures are cross-sections of the spinal cord of a control-RNAi transfected embryo, illustrating the different markers used to define Ts and Tc and to identify the proliferating population. Markers are indicated in each picture. (**G**) Schematic summary of the data obtained with these cell cycle kinetics analyses. (**H**) Table summarizing the durations of Tc, Ts and TG2 quantified in the present study; the mitosis length was estimated as about 30 minutes (Wilcock et al., 2007); the duration of the G1-phase length was calculated as the difference between Tc and (Ts+TG2+M). h, hours; min, minutes. **$P$<0.01, ***$P$<0.001.

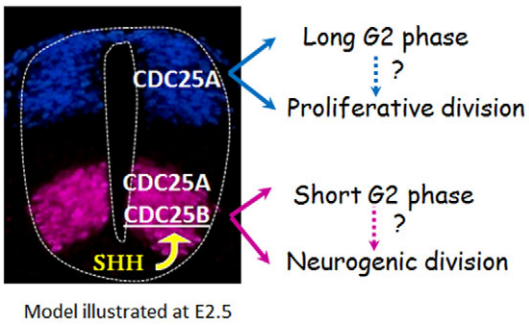


**Fig. 6. Model illustrating the role of CDC25B expression in neural progenitors.** In the chick dorsal spinal cord, only CDC25A is expressed, neural progenitors display a long G2 phase and perform proliferative divisions. In the ventral spinal cord, the Shh-dependent upregulation of CDC25B causes a shortening of the G2 phase and also promotes neurogenesis. Whether the shortening of the G2 phase is promoting neurogenesis remains to be elucidated.

this cell cycle parameter. Using the PLM method, we compared the G2-phase length under control conditions and after RNAi-based knock-down of CDC25B. Twenty-four hours after electroporation (analyses made at E2.5-E3; Fig. 5A,A′), downregulating *CDC25B* significantly delays the appearance of P-H3/BrdU-positive cells at each time point analyzed (Fig. 5B,B′), indicating that CDC25B influences G2-phase duration. The average G2 lengths of control versus CDC25B-RNAi-transfected progenitors deduced from the curve is 1 hour 27 minutes and 2 hours 7 minutes, respectively (Fig. 5B′). Furthermore, quantification of mitosis (P-H3) did not reveal a significant difference between embryos electroporated with CDC25B-RNAi (4.52±0.64%) and those electroporated with the control vector (5.24±0.56%; $P$=0.46) (Fig. 5E). This indicates that the difference in the percentage of labeled mitoses (Fig. 5B′) is mainly due to the difference in G2 length. Thus, misexpressing CDC25B in neural progenitors pushes them to enter mitosis rapidly (supplementary material Fig. S1E), whereas its downregulation delays mitotic entry, implying that the upregulation of CDC25B in neural progenitors results in a shorter G2 phase.

Last, we determined whether other parameters of the cell cycle were affected, in particular S phase, the progression of which can be modified by CDC25B downregulation (Garner-Hamrick and Fisher, 1998), and more generally whether CDC25B has an impact on total cell cycle length. To determine the length of S phase (Ts) and of the complete cell cycle (Tc), we used the BrdU/EdU double-labeling paradigm (Martynoga et al., 2005). BrdU/EdU double labeling was performed by in ovo application of BrdU followed by EdU for 2 hours and 30 minutes, respectively, prior to fixation (Fig. 5F). Quantification was performed on the proliferating region of the RFP+ population that was obtained by subtracting the number of HuC/D+-differentiated cells (RFP+/HuC/D+) from the total number of RFP+ transfected cells (Fig. 5F). The proportion of RFP+/BrdU+/EdU+ and RFP+/BrdU+/EdU– populations allows the Ts to be estimated (see Materials and methods). We did not detect a significant difference in the length of the S phase in the population of cells transfected with the control-RNAi (Ts=3 hours and 41±25 minutes, $n$=5 embryos, >2500 cells analyzed) compared with that transfected with the CDC25B-RNAi (Ts=3 hours and 4±29 minutes, $n$=5 embryos, >2200 cells analyzed; $P$=0.369) (Fig. 5G). We thought that the lack of Ts differences between the control- and CDC25B-RNAi populations could be due to dilution of the effect by the dorsal population. We thus restricted our quantification to the transgenic population located in the ventral third of the neural tube, but again we did not detect differences in Ts after CDC25B knockdown (4 hours and 3±53 minutes compared with 4 hours and 4±47 minutes in control; $P$=0.99). We also measured the total length of the cell cycle (Tc) but did not detect any significant difference between control-RNAi and CDC25B-RNAi-transfected cells (12 hours and 20 minutes±1 hour and 27 minutes compared with 11 hours and 4 minutes±1 hour and 20 minutes, respectively, $P$=0.536). Again, restricting the analysis to the ventral third of the neural tube did not reveal any differences (Tc=10 hours and 42 minutes±1 hours and 58 minutes versus 11 hours and 35 minutes ± 1 hours and 59 minutes in the control and CDC25B-RNAi-transfected embryos, respectively, $P$=0.78). Thus, CDC25B downregulation results in a lengthening of the G2 phase without significantly modifying the S phase or total cell cycle duration.

## DISCUSSION

We show that *CDC25A* is expressed in all proliferating progenitor domains of the developing spinal cord, whereas *CDC25B* expression correlates spatially and temporally with neurogenesis. We demonstrate that neural progenitors expressing both *CDC25A* and *CDC25B* display a shorter G2 phase than those expressing only *CDC25A*. Downregulating *CDC25B* lengthens the G2 phase, and this is associated with maintenance of the progenitor state at the expense of neuronal production. We propose a model in which combinatorial activity of CDC25A and CDC25B in neural progenitors shortens the G2 phase and adapts proliferation to the needs of neuron production (Fig. 6).

### The Shh-dependent upregulation of CDC25B expression in neural progenitors results in a shortening of the G2 phase

*CDC25B* transcription is initiated by Shh in the ventral neural tube at the onset of neurogenesis (Benazeraf et al., 2006). The co-expression of *CDC25A* and *CDC25B* correlates with domains where neural progenitors display a shorter G2 phase and probably a longer G1 phase, and where neurogenic activity is high (this study). It is thus tempting to propose that, under normal conditions, Shh controls cell cycle kinetics in part by modifying the level of the CDC25B phosphatase, in order to adapt it to the needs of neuronal production (Fig. 6). Mounting evidence indicates that cell cycle kinetics is determinant for the decision to leave the cell cycle and initiate differentiation. In *Xenopus* retina, Shh accelerates the cell cycle by reducing the lengths of G1 and G2 phases through activation of cyclin D1 and CDC25C, among other factors, thus converting stem cells to fast cycling progenitors that are closer to exiting the cell cycle (Locker et al., 2006). In the cortex, neuronal differentiation is associated with an increase in the cell cycle mainly due to a lengthening of the G1 phase (Dehay and Kennedy, 2007; Lange and Calegari, 2010) that accompanies the transition from apical to basal progenitors (Arai et al., 2011). Reducing the G1 phase in cortical progenitors impedes neurogenesis by promoting proliferative divisions (Lange et al., 2009; Pilaz et al., 2009). Finally, apical and basal progenitors committed to neuronal differentiation display a shorter S phase than those undergoing proliferative divisions, whereas G1-phase length is unchanged (Arai et al., 2011). In the chicken neural tube, cell divisions generating neurons have been shown to have a longer cell cycle than those generating progenitors (Wilcock et al., 2007). We did not detect any significant changes in total cell cycle duration in neural progenitors following CDC25B downregulation. This apparent discrepancy may just be

methodological, as we defined total cell cycle length globally, in a heterogeneous population of progenitors performing proliferative and neurogenic divisions, whereas it was previously measured in single progenitors using time-lapse imaging in embryo slice cultures (Wilcock et al., 2007). We nevertheless observed that domains containing progenitors undergoing neurogenic divisions have a shortened G2 phase, and that CDC25B downregulation modifies both the length of the G2 phase and also neuronal production. This tight correlation between G2-phase duration and neurogenesis strongly suggests that shortening the G2 phase, possibly in association with lengthening the G1 phase is a key step in the sequence of events that allows a neural progenitor to undergo neurogenic divisions and thus differentiate. The challenge is now to dissect the causal relationship between the two events.

## CDC25B and the paradox of a positive cell cycle regulator that promotes neuronal differentiation

We show here that knocking down CDC25B in the neural tube results in an increase in the number of progenitors and a decrease in the number of neurons, indicating that CDC25B acts as a positive regulator of differentiation. A study performed during early *Xenopus* development showed that in neurectoderm, cell-cycle progression mediated by FoxM1 or its target G2-M regulators, including CDC25B, is essential for neuronal differentiation, which corroborates our findings (Ueno et al., 2008). We demonstrate that downregulating CDC25B results in a delayed G2/M transition. How could a modification in the length of the G2 phase affect the decision of a neural progenitor to differentiate? Based on data in the literature, several scenarios can be proposed. In *Drosophila* wing disc, an alteration in the length of one cell cycle phase can be compensated by a modification of another phase, in order to maintain a normal rate of division (Reis and Edgar, 2004). Thus, in our model, the shortening of the G2 phase might be compensated by a lengthening of the G1 phase in the daughter cells (see Fig. 5H) without affecting the rate of division at the time of intensive neuron production. Analyses of the primary microcephaly gene 1 (MCPH1) function in mouse cortex, reveal that alterations of the Chk1-CDC25B-Cdk1 pathway uncouple the centrosome cycle from entry into mitosis, leading to inaccurate mitotic spindle orientation that promotes asymmetric divisions and neurogenesis (Gruber et al., 2011). Interestingly, the MCPH1 mutation induces an increase of CDC25B activity, and silencing CDC25B in this context rescues the phenotype of precocious neuronal differentiation, a result that fits well with our observations. Upregulation of CDC25B in spinal progenitors could modify the synchrony between centrosome maturation and the timing of entry into mitosis in a way that favors neurogenic divisions. Various signaling pathways have a predominant function at the G2/M boundary. The Notch signaling pathway is known to maintain cells in the progenitor state, and accumulating evidence reveals a preferential activation of Notch in progenitors about to enter mitosis (Cisneros et al., 2008; Murciano et al., 2002; Vilas-Boas et al., 2011). Thus, a longer G2/M transition may lengthen the exposure of spinal progenitors to high levels of Notch signaling and thus influence their decision to differentiate. The Wnt pathway is also well known for its capacity to keep neural progenitors proliferating in the developing spinal cord (Megason and McMahon, 2002). Wnt/β-catenin signaling is influenced by the cell cycle, its activity peaking at the G2/M transition (Davidson et al., 2009). Moreover, disrupting the three CDC25 genes by homologous recombination in the mouse small intestine results in enhanced Wnt/β-catenin signaling (Lee et al., 2009). Thus, a shortening of the G2 phase in spinal progenitors in response to CDC25B phosphatase activity could diminish their sensitivity to the Wnt pathway and favor neuron differentiation. Finally, CDC25B persists in young neurons (see Fig. 1O, CDC25B-NeuroM), possibly promoting neurogenesis in a cell cycle-independent manner, as shown for other cell cycle regulators (Lukaszewicz and Anderson, 2011). Deciphering the mechanisms underlying CDC25B function in neurogenesis is therefore a challenging point that remains to be elucidated.

In conclusion, we propose that during the period when the morphogen Shh controls cell fate in the spinal cord, this signaling pathway activates expression of the cell cycle regulator CDC25B (Benazeraf et al., 2006). Increasing the phosphatase activity in neural progenitors has two functions: it shortens the G2 phase and also allows efficient differentiation of specified neuronal precursors (Fig. 6). This scenario may also be involved in numerous organs where Shh has pleiotropic effects, i.e. specification, proliferation and differentiation.

**Acknowledgements**

We thank Dr J. Muhr for the gift of NeuroM antibodies; S. Bel-Vialar, P. Cochard, M. Crozatier, A. Davy, C. Monod-Wissler, J. Smith and C. Soula for helpful comments on the manuscript; C. Dozier for helping with western blots; C. Andalo for helping with statistical analyses; and A. Le Ru and B. Ronsin for technical assistance in confocal microscopy on the Toulouse RIO imaging platform.

**Funding**

This work was supported by the Centre National de la Recherche Scientifique, le Ministère de l'Education Nationale et de la recherche, la ligue contre le cancer to B.D. (Equipe labellisée 2008) and by l'Association Française contre les Myopathies (AFM). E.P. was a recipient of the PhD fellowship from AFM.

**Competing interests statement**

The authors declare no competing financial interests.

**Supplementary material**

Supplementary material available online at
http://dev.biologists.org/lookup/suppl/doi:10.1242/dev.068569/-/DC1

**References**

**Agathocleous, M., Locker, M., Harris, W. A. and Perron, M.** (2007). A general role of hedgehog in the regulation of proliferation. *Cell Cycle* **6**, 156-159.
**Akai, J., Halley, P. A. and Storey, K. G.** (2005). FGF-dependent Notch signaling maintains the spinal cord stem zone. *Genes Dev.* **19**, 2877-2887.
**Alvarez-Medina, R., Le Dreau, G., Ros, M. and Marti, E.** (2009). Hedgehog activation is required upstream of Wnt signalling to control neural progenitor proliferation. *Development* **136**, 3301-3309.
**Arai, Y., Pulvers, J. N., Haffner, C., Schilling, B., Nusslein, I., Calegari, F. and Huttner, W. B.** (2011). Neural stem and progenitor cells shorten S-phase on commitment to neuron production. *Nat. Commun.* **2**, 154.
**Bel-Vialar, S., Medevielle, F. and Pituello, F.** (2007). The on/off of Pax6 controls the tempo of neuronal differentiation in the developing spinal cord. *Dev. Biol.* **305**, 659-673.
**Benazeraf, B., Chen, Q., Peco, E., Lobjois, V., Medevielle, F., Ducommun, B. and Pituello, F.** (2006). Identification of an unexpected link between the Shh pathway and a G2/M regulator, the phosphatase CDC25B. *Dev. Biol.* **294**, 133-147.
**Boutros, R., Lobjois, V. and Ducommun, B.** (2007). CDC25 phosphatases in cancer cells: key players? Good targets? *Nat. Rev. Cancer* **7**, 495-507.
**Bugler, B., Schmitt, E., Aressy, B. and Ducommun, B.** (2010). Unscheduled expression of CDC25B in S-phase leads to replicative stress and DNA damage. *Mol. Cancer* **9**, 29.
**Cayuso, J., Ulloa, F., Cox, B., Briscoe, J. and Marti, E.** (2006). The Sonic hedgehog pathway independently controls the patterning, proliferation and survival of neuroepithelial cells by regulating Gli activity. *Development* **133**, 517-528.
**Cisneros, E., Latasa, M. J., Garcia-Flores, M. and Frade, J. M.** (2008). Instability of Notch1 and Delta1 mRNAs and reduced Notch activity in vertebrate neuroepithelial cells undergoing S-phase. *Mol. Cell Neurosci.* **37**, 820-831.
**Das, R. M., Van Hateren, N. J., Howell, G. R., Farrell, E. R., Bangs, F. K., Porteous, V. C., Manning, E. M., McGrew, M. J., Ohyama, K., Sacco, M. A. et al.** (2006). A robust system for RNA interference in the chicken using a modified microRNA operon. *Dev. Biol.* **294**, 554-563.
**Davidson, G., Shen, J., Huang, Y. L., Su, Y., Karaulanov, E., Bartscherer, K., Hassler, C., Stannek, P., Boutros, M. and Niehrs, C.** (2009). Cell cycle control of wnt receptor activation. *Dev. Cell* **17**, 788-799.

**Dehay, C. and Kennedy, H.** (2007). Cell-cycle control and cortical development. *Nat. Rev. Neurosci.* **8**, 438-450.
**Dessaud, E., McMahon, A. P. and Briscoe, J.** (2008). Pattern formation in the vertebrate neural tube: a sonic hedgehog morphogen-regulated transcriptional network. *Development* **135**, 2489-2503.
**Garner-Hamrick, P. A. and Fisher, C.** (1998). Antisense phosphorothioate oligonucleotides specifically down-regulate cdc25B causing S-phase delay and persistent antiproliferative effects. *Int. J. Cancer* **76**, 720-728.
**Gruber, R., Zhou, Z., Sukchev, M., Joerss, T., Frappart, P. O. and Wang, Z. Q.** (2011). MCPH1 regulates the neuroprogenitor division mode by coupling the centrosomal cycle with mitotic entry through the Chk1-Cdc25 pathway. *Nat. Cell Biol.* **13**, 1325-1323.
**Hamburger, V. and Hamilton, H. L.** (1992). A series of normal stages in the development of the chick embryo. 1951. *Dev. Dyn.* **195**, 231-272.
**Hammerle, B. and Tejedor, F. J.** (2007). A novel function of DELTA-NOTCH signalling mediates the transition from proliferation to neurogenesis in neural progenitor cells. *PLoS ONE* **2**, e1169.
**Karlsson, C., Katich, S., Hagting, A., Hoffmann, I. and Pines, J.** (1999). Cdc25B and Cdc25C differ markedly in their properties as initiators of mitosis. *J. Cell Biol.* **146**, 573-584.
**Lange, C. and Calegari, F.** (2010). Cdks and cyclins link G(1) length and differentiation of embryonic, neural and hematopoietic stem cells. *Cell Cycle* **9**, 1893-1900.
**Lange, C., Huttner, W. B. and Calegari, F.** (2009). Cdk4/cyclinD1 overexpression in neural stem cells shortens G1, delays neurogenesis, and promotes the generation and expansion of basal progenitors. *Cell Stem Cell* **5**, 320-331.
**Lee, G., White, L. S., Hurov, K. E., Stappenbeck, T. S. and Piwnica-Worms, H.** (2009). Response of small intestinal epithelial cells to acute disruption of cell division through CDC25 deletion. *Proc. Natl. Acad. Sci. USA* **106**, 4701-4706.
**Lobjois, V., Benazeraf, B., Bertrand, N., Medevielle, F. and Pituello, F.** (2004). Specific regulation of cyclins D1 and D2 by FGF and Shh signaling coordinates cell cycle progression, patterning, and differentiation during early steps of spinal cord development. *Dev. Biol.* **273**, 195-209.
**Lobjois, V., Bel-Vialar, S., Trousse, F. and Pituello, F.** (2008). Forcing neural progenitor cells to cycle is insufficient to alter cell-fate decision and timing of neuronal differentiation in the spinal cord. *Neural Dev.* **3**, 4.
**Lobjois, V., Jullien, D., Bouche, J. P. and Ducommun, B.** (2009). The polo-like kinase 1 regulates CDC25B-dependent mitosis entry. *Biochim. Biophys. Acta* **1793**, 462-468.
**Locker, M., Agathocleous, M., Amato, M. A., Parain, K., Harris, W. A. and Perron, M.** (2006). Hedgehog signaling and the retina: insights into the mechanisms controlling the proliferative properties of neural precursors. *Genes Dev.* **20**, 3036-3048.
**Lukaszewicz, A. I. and Anderson, D. J.** (2011). Cyclin D1 promotes neurogenesis in the developing spinal cord in a cell cycle-independent manner. *Proc. Natl. Acad. Sci. USA* **108**, 11632-11637.
**Martynoga, B., Morrison, H., Price, D. J. and Mason, J. O.** (2005). Foxg1 is required for specification of ventral telencephalon and region-specific regulation of dorsal telencephalic precursor proliferation and apoptosis. *Dev. Biol.* **283**, 113-127.
**Megason, S. G. and McMahon, A. P.** (2002). A mitogen gradient of dorsal midline Wnts organizes growth in the CNS. *Development* **129**, 2087-2098.
**Morin, X., Jaouen, F. and Durbec, P.** (2007). Control of planar divisions by the G-protein regulator LGN maintains progenitors in the chick neuroepithelium. *Nat. Neurosci.* **10**, 1440-1448.
**Murciano, A., Zamora, J., Lopez-Sanchez, J. and Frade, J. M.** (2002). Interkinetic nuclear movement may provide spatial clues to the regulation of neurogenesis. *Mol. Cell Neurosci.* **21**, 285-300.
**Pilaz, L. J., Patti, D., Marcy, G., Ollier, E., Pfister, S., Douglas, R. J., Betizeau, M., Gautier, E., Cortay, V., Doerflinger, N. et al.** (2009). Forced G1-phase reduction alters mode of division, neuron number, and laminar phenotype in the cerebral cortex. *Proc. Natl. Acad. Sci. USA* **106**, 21924-21929.
**Pituello, F., Yamada, G. and Gruss, P.** (1995). Activin A inhibits Pax-6 expression and perturbs cell differentiation in the developing spinal cord in vitro. *Proc. Natl. Acad. Sci. USA* **92**, 6952-6956.
**Quastler, H. and Sherman, F. G.** (1959). Cell population kinetics in the intestinal epithelium of the mouse. *Exp. Cell Res.* **17**, 420-438.
**Reis, T. and Edgar, B. A.** (2004). Negative regulation of dE2F1 by cyclin-dependent kinases controls cell cycle timing. *Cell* **117**, 253-264.
**Rivers, D. M., Moreno, S., Abraham, M. and Ahringer, J.** (2008). PAR proteins direct asymmetry of the cell cycle regulators Polo-like kinase and Cdc25. *J. Cell Biol.* **180**, 877-885.
**Rowitch, D. H.** (2004). Glial specification in the vertebrate neural tube. *Nat. Rev. Neurosci.* **5**, 409-419.
**Sockanathan, S. and Jessell, T. M.** (1998). Motor neuron-derived retinoid signaling specifies the subtype identity of spinal motor neurons. *Cell* **94**, 503-514.
**Timofeev, O., Cizmecioglu, O., Hu, E., Orlik, T. and Hoffmann, I.** (2009). Human Cdc25A phosphatase has a non-redundant function in G2 phase by activating Cyclin A-dependent kinases. *FEBS Lett.* **583**, 841-847.
**Timofeev, O., Cizmecioglu, O., Settele, F., Kempf, T. and Hoffmann, I.** (2010). Cdc25 phosphatases are required for timely assembly of CDK1-cyclin B at the G2/M transition. *J. Biol. Chem.* **285**, 16978-16990.
**Ueno, H., Nakajo, N., Watanabe, M., Isoda, M. and Sagata, N.** (2008). FoxM1-driven cell division is required for neuronal differentiation in early Xenopus embryos. *Development* **135**, 2023-2030.
**Ulloa, F. and Briscoe, J.** (2007). Morphogens and the control of cell proliferation and patterning in the spinal cord. *Cell Cycle* **6**, 2640-2649.
**Vilas-Boas, F., Fior, R., Swedlow, J. R., Storey, K. G. and Henrique, D.** (2011). A novel reporter of notch signalling indicates regulated and random notch activation during vertebrate neurogenesis. *BMC Biol.* **9**, 58.
**Wilcock, A. C., Swedlow, J. R. and Storey, K. G.** (2007). Mitotic spindle orientation distinguishes stem cell and terminal modes of neuron production in the early spinal cord. *Development* **134**, 1943-1954.